Investigation of Low-Energy Plasma in the Earth's Magnetosphere onboard the *Tail* and *Auroral Probes*: Instrumentation and Preliminary Results

V. V. Bezrukikh*, N. A. Barabanov**, Yu. I. Venediktov**, V. I. Zhdanov*, V. I. Ivchenko***, G. A. Kotova*, L. A. Lezhen*, S. A. Orzhinskii**, and V. I. Prokhorenko*

*Space Research Institute, Russian Academy of Sciences, Profsoyuznaya ul. 84/32, Moscow, 117810 Russia
**Odessa Polytechnical University, Odessa, Ukraine
***Shevchenko State University, ul. Glushkova 6, Kiev, 252127 Ukraine
Received July 10, 1997

Abstract—We present a brief description and the parameters of the ALFA-3 instrument installed onboard the *Tail Probe* and *Auroral Probe* for local measurements of the characteristics of low-energy plasma and for a study started during the *Luna-2* and *Luna-3* missions [1, 2] of the spatial distribution of plasma in the Earth's magnetosphere. Some of the preliminary results obtained with this instrument inside and outside the plasmasphere at middle and high latitudes are also discussed.

INSTRUMENTATION

The ALFA-3 instrument was installed onboard the *Tail Probe* and *Auroral Probe* to measure the characteristics and energy spectra of ion fluxes with energies 0–25.5 eV and to study the spatial distribution of cold ions in the Earth's magnetosphere.

The instrument consists of the following units:

(1) A plane electrostatic analyzer of the PL-48 (RPA) type with retarding potential, which is mounted on the frame of the measuring direct-current amplifier;

(2) A plane electrostatic modulating analyzer of the PL-19 (MPA) type with a quasi-resonance amplifier built in the special compartment of the analyzer frame and tuned to the modulation frequency;

(3) An electronic AP-3 unit providing the required modes of analyzer operation and signal exchange with satellite service systems.

At both satellites, these two analyzers are installed on the nonsunlit satellite surface and oriented antisunward. The normals to the surface of the entrance windows are parallel to the satellite rotation axis. If we disregard the deviation of the satellite rotation axis from the sunward direction, which may reach several degrees, we can consider, with allowance for the width of the analyzer's angular diagram, that the two analyzers are oriented along the $-X$ axis of the solar-ecliptic coordinate system. The nonsunlit arrangement of the two analyzers ruled out the direct action of solar ultraviolet radiation on their readings.

The electric scheme of the PL-48 analyzer is shown in Fig. 1a. Entrance grid *1* and screen grids *3*

and *4* are connected with the analyzer frame. Suppressor grid *5* is kept at the –40 V potential. The voltage $U_a = 0–25.5$ V is applied to the analyzing double-grid electrode *2*.

All grids are made of nickel-plated tungsten wire 0.02 mm in diameter. Collector *C* made of a nickel plate 0.5 mm thick is kept at a negative potential of –20 V. The potentials of all electrodes are measured relative to the analyzer frame.

The current-voltage characteristic of the PL-48 analyzer, i.e., the dependence of analyzer current on the potential U at the analyzing grid and on the angle A between the ion flux direction and the normal to the entrance window, is plotted in Fig. 1b. The currents are normalized to the current value at $A = 0°$, and the potentials are normalized to the E/e value, where E is the ion beam energy, and e is the electron charge.

The main technical parameters of the PL-48 analyzer are the following:

Energy range of measured fluxes	0–25.5 eV;
Number of energy intervals	24;
Energy interval width	0.1–3.2 eV;
Range of measured fluxes	$10^5–10^9$ cm^{-2} s^{-1};
Effective collector area	10.56 cm^2;
Width of angular diagram	±60°;
Spectrum measuring time	1.8 s.

It should be noted that the AC current from the PL-48 collector is recorded in flight as a function of AC potential at the analyzing grid, and, therefore, the analyzer's

(a)

Arb. units (b)
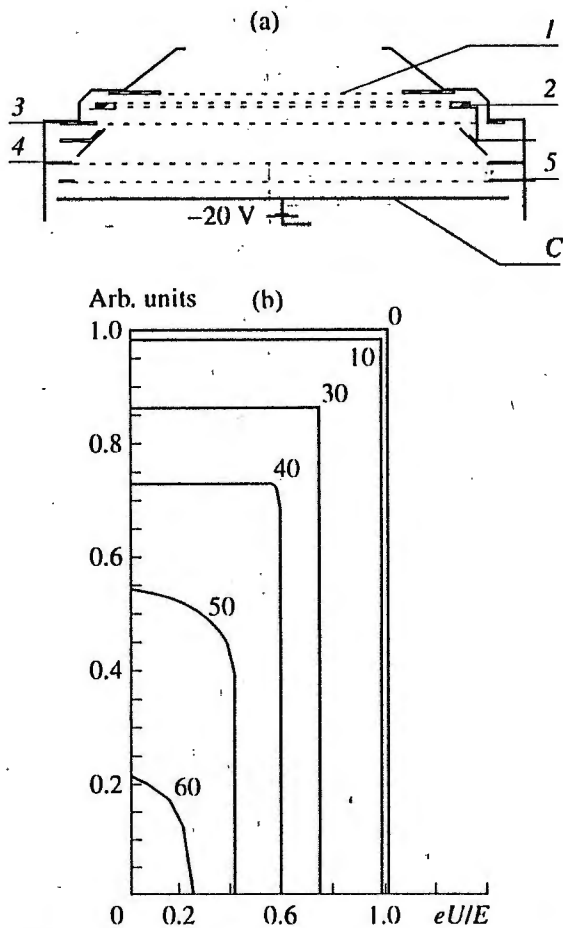
Fig. 1. (a) Schematic view of the PL-48 analyzer; (b) current–voltage characteristic of the PL-48 analyzer, which gives the dependence of the analyzer current on the potential U at the analyzing grid and on the angle of attack (angle between the direction of the ion flux and the normal to the analyzer entrance window).

(a)

(b)

Arb. units

Fig. 2. (a) Schematic view of the PL-19 analyzer; (b) current–voltage characteristics of the PL-19 analyzer.

output is not the retardation curve (occasionally called the integral spectrum) but the differential spectrum. Simultaneously, as the energy spectrum is measured, the total flux of charged particles in the analyzer collector circuit is also measured. Only ions with $E > U_{SC}$ (where U_{SC} is the positive spacecraft potential) and electrons with $E > 40$ eV (if the negative potential $U_{SC} < 40$ eV) can reach the collector C.

The schematic view of the PL-19 analyzer is presented in Fig. 2a. Grid 1 is placed in the analyzer window. In the experiment considered, grid 1 is conductively coupled with the analyzer frame. Electrode system 2 is designed to provide a change of the analyzer's angular diagram. In the course of experiment, electrode 2 is connected up alternately either with the analyzer frame or with analyzing electrode 4 via the voltage divider. Screen grid 3 and screen package 5 are connected with the analyzer frame. The screen package, consisting of 5 interconnected grids, provides complete electrostatic insulation of analyzing grid 4

from collector C. Figure 2b shows the current–voltage characteristics of the PL-19 analyzer for the two variants of electrode 2 connection ($U_2 = 0$ V on the left, and $U_2 = 0.9U_a$ on the right).

The energy range of measured fluxes, the number and width of energy intervals, the range of measured fluxes, and the spectrum measuring time coincide with similar parameters for the PL-48 analyzer. The widths of angular diagrams for the first and second modes of the PL-19 operation are $\pm 50°$ and $\pm 40°$, respectively. The collector effective area is 11.3 cm^2.

The complete telemetry frame from the ALFA-3 instrument contains 3 energy spectra: the spectrum measured by the PL-48 analyzer and two spectra measured by the PL-19 analyzer in two modes.

Energy spectra are measured by the PL-48 analyzer with the following procedure:

1. The presence of a measurable ion flux with energies 0–25.5 eV is determined;

2. If an ion flux is revealed in the above energy range, the voltage U_b at the analyzing grid is measured, at which the analyzer begins to detect the current increase in response to the change of the analyzing voltage. The voltage U_b, which determines the position of the ion flux spectrum on the energy scale, can be varied in the range 0–25.5 V with a step of 0.1 V. The combined voltage $U_a = U_b + U_s$ is applied to the analyzing grid, with the scanning voltage U_s variable from 0 to 25.5 V. The voltage U_a does not exceed 25.5 V. The scanning voltage U_s is grouped into 6 groups of 4 steps each. In the first group, the scanning voltage varies in 0.1 V steps. In each subsequent

Ion fluxes, 10^5 cm^{-2} s^{-1}
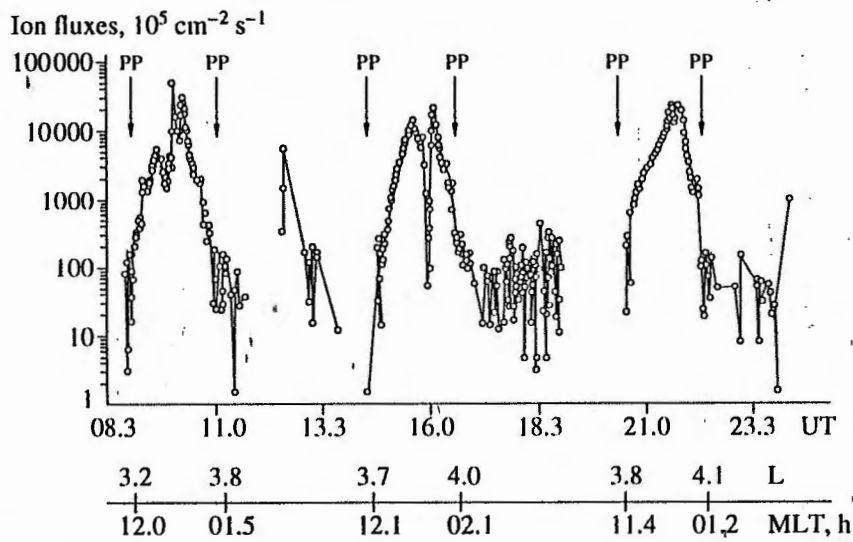
Fig. 3. Ion fluxes recorded on September 14, 1996, in three successive orbits of the *Auroral Probe*.

group, this voltage step is doubled. In the last group, the scanning voltage step is 3.2 V. For each analyzing voltage, currents are measured in the analyzer collector circuit. The spectrum measurement ends when the measured current falls below the sensitivity limit or when the analyzing voltage reaches the value $U_a = U_b + U_s = 25.5$ V; after that, the measuring cycle in the PL-19 analyzer begins.

3. If the collector amplifier in the PL-48 analyzer does not measure current in the process of energy scanning, the PL-19 analyzer begins its measurements.

Measurements with the PL-19 analyzer are carried out with the use of a similar algorithm, except that in this case, the analyzing voltage is $U_a = U_b + U_s + U_m$, where U_m is the modulating rectangular voltage with a frequency of 500 Hz, the full swing of which is equal to the difference between the given and subsequent U_s values. With this choice of modulating voltage, the differential spectra are also recorded by the PL-19 analyzer.

When measuring the energy spectra by each analyzer, the following data are transmitted to the telemetry system:

the conventional code of each analyzer;

the voltage U_b, specifying the position of the ion flux spectrum on the energy scale;

the current value in every energy interval; and

the number of the scale used by the current amplifier.

In addition, the magnitude and sign of the total current of the PL-48 collector at $U_a = 0$ V is transmitted to the telemetry system.

MEASUREMENT RESULTS AND DISCUSSION

Below we give and discuss the results of measurements obtained with the PL-19 analyzer onboard the *Auroral Probe* during the period September 9–14, 1996, which are typical for the September–October period of 1996. We consider separately the results of measurements in the plasmapause, in the outside region adjacent to the plasmapause, and at geocentric distances $4R_E$ above the polar cap.

Measurements in the Plasmasphere and Exoplasmasphere

The results of measurements of ion fluxes in the energy range 0–25.5 eV from 08:40 to 23:50 UT on September 14, 1996, as a function of the Universal Time are shown in Fig. 3. The maximum fluxes, which may be as high as 2×10^9–5×10^9 cm^{-2} s^{-1}, are detected near the orbit perigee. The dramatic fluctuations of ion fluxes observed at ~10:00 UT and especially at ~16:00 UT are explained by the probe passage through a region of high latitudes and the polar cap; they are related to fluctuations of cold plasma concentration. It is also evident from Fig. 3 that the smooth variation of measured flux values before and after the passage of the perigee by *Auroral Probe* (during the probe flight across the plasmasphere) is accompanied every time by a sharp decrease in measured fluxes. The decrease in fluxes can be explained by the probe passage through the plasmapause. Positions of the plasmapause, which were determined by the sharp decrease or increase of the ion flux recorded by the instrument, are marked in Fig. 3 by arrows, while the values of the L coordinate and local time corresponding to the plasmapause positions are plotted on the lower axis. The positions of the plasma-

September 14, 1996
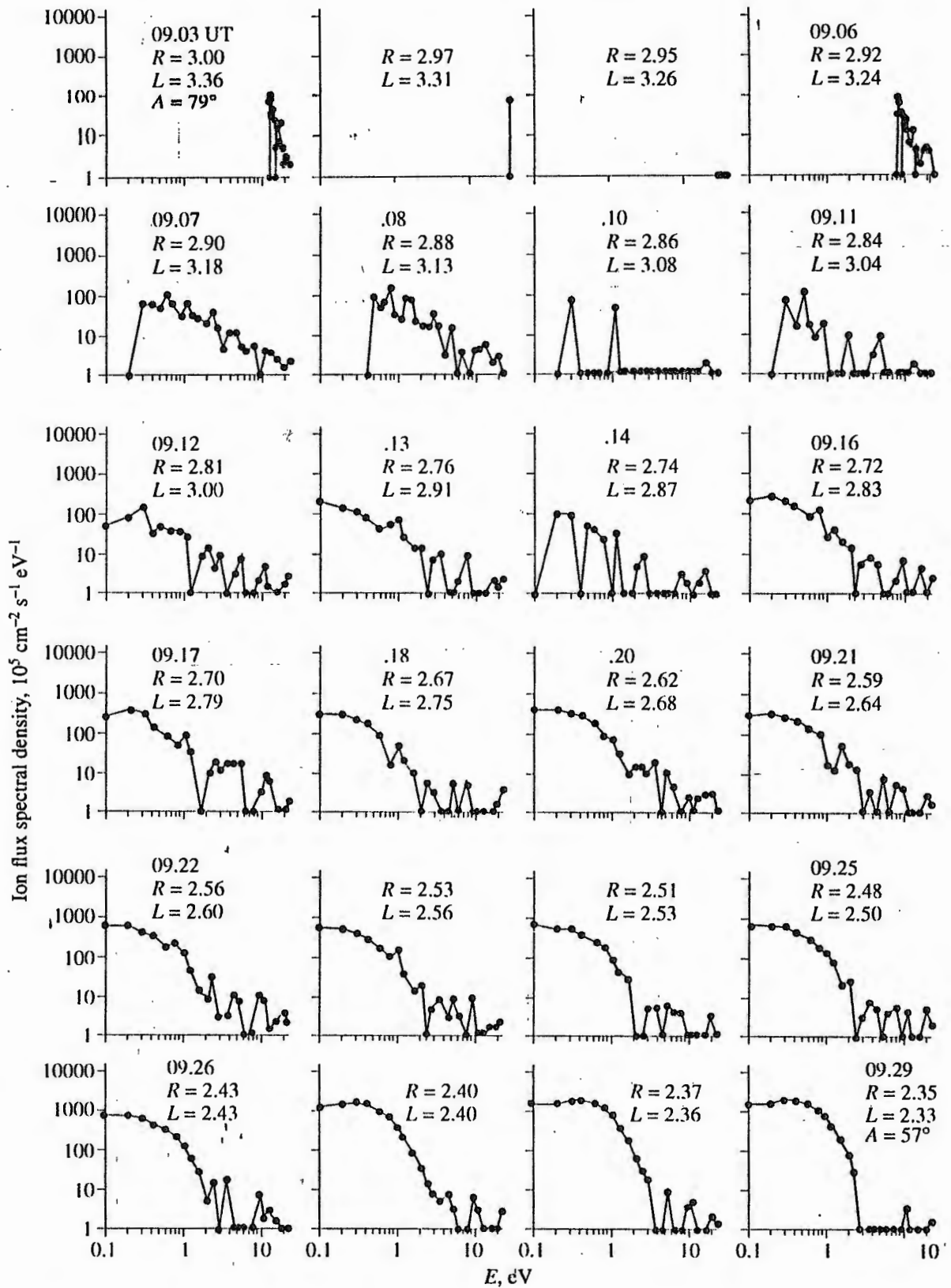
Fig. 4. Energy spectra measured outside (at 09:03–09:06 UT) and inside the plasmasphere (at 09:07–09:29 UT).

pause detected by the ALFA-3 instrument on September 14, 1996, correspond to the phase of refilling of the plasmasphere with ionospheric plasma after its depletion, which was likely to occur at the period of two intensive substorms on September 12, 1996, and on September 13, 1996, when the K_{pm} (maximum K_p) value was 5_- and 5_0, respectively.

The data in Fig. 3 make it possible to estimate the rate of refilling of the plasmasphere and the shift of the plasmapause onto the more distant L shells, which is related to such refilling: in 18 hours of measurements, the plasmapause in the noon sector shifted from $L = 3.2$ to $L = 3.7$, and in the midnight sector, from $L = 3.8$ to $L = 4.1$.

Outside the plasmasphere (in the magnetospheric region located between the plasmapause and the plasma sheet, which is currently called "exoplasmasphere"), heavily fluctuating ion fluxes are measured by the instrument, whose values, as a rule, range from 2×10^6–3×10^7 cm^{-2} s^{-1} and only occasionally, near the apogee at $R = 4R_E$ and $L > 9$, reach the values 10^8–10^9 cm^{-2} s^{-1}.

Before proceeding to the examination of the results of spectral measurements of cold ion fluxes, we consider it necessary to dwell on the problem of the dependence of the results of the measurements of low-energy plasma on the satellite potential. The effect of the SC potential on the results of measuring the cold plasma manifests itself, on the one hand, in the change near the SC of the local density of charged particles with energies $E \sim eU_{SC}$, where U_{SC} is the SC potential [3, 4] and, on the other hand, leads to the shift of the measured energy spectra along the energy axis. The positive potential moves the ion spectrum toward lower energies, while the negative potential, toward higher energies. Moreover, the positive SC potential, whose value $U_{SC} \sim (3-5)kT/e$ (here k is the Boltzmann constant, T is the absolute temperature, and e is the electron charge), or 1–3 V, may cause the effect of so called "hidden" plasma [5]. This effect manifests itself in that the cold plasma, which really exists near the SC having a positive potential with respect to the ambient medium, remains "invisible" to onboard instruments. It is known that the SC potential is formed primarily under the influence of the fluxes of charged particles and electromagnetic radiation acting upon the SC. It is also known that the U_{SC} depends on many "technological" factors: the SC frame material, surface treatment and surface conditions, the type of coating, etc. The theoretical estimates and experimental data obtained from many experiments in the ionosphere and plasmasphere [4] show that U_{SC} usually varies from a few tenths of a volt to a few volts, and its sign is negative. As the SC travels toward the plasmapause, the absolute U_{SC} value decreases and tends to zero near the plasmapause. Outside the plasmasphere, but near it, the U_{SC} values are also small, but the sign of U_{SC} is often positive. For example, the poten-

tial of the geostationary satellites *GEOS* and *SCATHA* was, according to [6], close to $+3$ V, with the *GEOS* potential variations from $+3$ V to $+8$ V; and the potential of the *ISEE* satellite was positive in the solar wind, in the magnetosheath, and in the magnetosphere (outside the plasmasphere) [7]. However, in the plasma sheet, U_{SC} may become negative and reach significant values. On the *ATS-5*, *ATS-6*, and *SCATHA* satellites, when they were in the Earth's shadow cone, the potentials as high as a few kiloelectronvolts were measured [4, 8].

The surface of *Auroral Probe* was metallized, which excluded the effect of differential charging of the SC surface. The preliminary analysis of the energy spectra of cold plasma, measured at the period from September 09, 1996, to September 11, 1996, shows that in the plasmasphere, U_{SC} was close to zero. In any case, its value was not higher than 0.5 V, and its sign was, as a rule, negative.

Figure 4 displays a series of differential energy spectra of ion fluxes measured by the *ALFA-3* instrument on the inbound leg of the orbit on September 14, 1996, when *Auroral Probe* crossed successively the exoplasmasphere, plasmapause, and plasmasphere in the noon sector of the magnetosphere from 09:03 UT to 09:29 UT. The day of September 14 is characterized by a moderate geomagnetic disturbance, when $K_{pm} = 3$ (K_{pm} is the maximum value of the K_p index on the day of measurements); however, on September 13, 1996, we had $K_{pm} = 5_-$, and on September 12, 1996, we had $K_{pm} = 5_+$. In connection with this, we may assume that the measurements on September 14, 1996, were made at the time of filling of field tubes with ionospheric plasma after their devastation caused by intensive substorms on September 12, 1996, and September 13, 1996. At that period, the satellite velocity V_{SC} was in the range 4.1–5.4 km s^{-1}, and the angle of attack A (angle between the normal to the entrance window and the direction of satellite flight) varied from 78° at 09:03 UT spectrum measurement to 57° at 09:29 UT measurement. For each spectrum shown in Fig. 4, we give the initial time of spectrum measurement, and the corresponding geocentric distance R_E and the L coordinate. For the first and the last spectra, the angles A are also indicated. The results of measurements shown in Fig. 4 allow us to make the following conclusions:

1. At the time interval 09:03–09:06 UT, the analyzer measures only ion fluxes with $E > 9$ eV; their value varies from 10^5 to 10^7 cm^{-2} s^{-1} eV^{-1};

2. Between 09:06 and 09:07 UT, the flux of ions with $E < 25.5$ eV sharply increases up to 10^8 cm^{-2} s^{-1} eV^{-1}; in this case, the maxima in the spectrum are shifted to $E < 1$ eV. These dramatic changes in the flux value and the position of the spectrum on the energy axis are accounted for by the satellite's crossing of the plasmapause; they are typical for the crossing of the plasmapause by *Tail Probe* and *Auroral Probe* in the nightside, dawn, and dayside sectors of the magnetosphere.

As follows from the above discussion, the shift of the maximum in the measured ion flux spectra toward higher energies, when going from the plasmasphere to the exoplasmasphere, cannot be explained by decreasing U_{SC} down to -20 eV. Thus, the high-energy shift of the maximum in crossing the plasmapause on the outbound legs of satellite orbits may be caused by an increase in the energy of directed motion of the low-energy plasma with the velocity component perpendicular to the entrance window. Since the analyzers installed onboard the Tail and Auroral Probes are oriented antisunward, the low-energy ion fluxes have a velocity component V_x in solar-ecliptic coordinate system corresponding to the energy $9 \leq E \leq 25.5$ eV. We believe that outside the plasmasphere, the fluxes of low-energy ions with energy between 9 and 25 eV, which presumably take part in the large-scale magnetospheric convection, are recorded with the ALFA-3 instrument, and the region where convective fluxes of low-energy plasma are detected adjoins directly to the plasmapause. The descending shape of the spectra measured outside the plasmasphere suggests that the ion fluxes are generated by ions of atmospheric origin. The last conclusion agrees well with the viewpoint that low-energy plasma of atmospheric origin is quite abundant in the Earth's magnetosphere and is an essential component of the large-scale structures of the terrestrial magnetosphere [10, 11]. The density of low-energy ions outside the plasmasphere at low and middle latitudes is $1-3$ cm^{-3}, which is reasonably consistent with the results obtained in [6, 9, 12].

It is also evident from Fig. 4 that, inside the plasmasphere, immediately after the plasmapause crossing, from 09:07 to 09:17 UT ($3.18 > L > 2.79$), the shape of the measured spectra differs significantly from the Maxwellian distribution. Beginning from 09:18 UT ($L < 2.75$), the shape of the measured spectra agrees quite satisfactorily with the Maxwellian distribution.

Analysis of experimental data obtained in September–October of 1996 at different levels of geomagnetic disturbance shows that the existence in the plasmasphere of a region adjacent to the plasmapause where the energy distribution of ions differs substantially from the Maxwellian seems to be a permanent feature of the plasmasphere, although the L coordinate of the inner boundary may vary over wide limits. The existence of this region is possibly related to the processes described in [13, 14], which attend the filling of geomagnetic tubes with ionospheric plasma after their devastation caused by geomagnetic disturbances. It should be stressed that, according to [15], the data obtained by the DE-1 satellite indicate that, within a day after the decline of the level of geomagnetic disturbance, the new ionospheric plasma refilling previously depleted field tubes had near-Maxwellian energy distribution.

Measurements at Geocentric Distances $4R_E$ above the Polar Cap

It is known that the concept of the polar wind was suggested by Axford [16], and by Banks and Holzer [17] in 1968. However, it is likely that the first measurements of the polar wind were only made 12 years later by Hoffman and Dodson [18]. Systematic experimental data concerning the polar wind were obtained on the DE satellites. These data were used as the basis for constructing the model of the polar wind known as the "cleft ion fountain" or "geomagnetic mass-spectrometer" model [19, 20]. The authors of this model considered the flux of the polar wind to consist of a mixture of H$^+$, He$^+$, and O$^+$ ions with allowance for the longitudinal (ambipolar) and transverse (convection) electric fields in the Earth's gravitational field. According to the above model, the flux of the polar wind from the nightside sector, which initially consisted of the mixture of three light ions, begins to split at altitudes $\sim 1.5R_E$ under the action of gravity. At first, O$^+$ ion fluxes, at higher altitudes, He$^+$ fluxes, and at still higher altitudes, proton fluxes separate from it. The fluxes of O$^+$ ions fall in the region of the plasma sheet nearest to the Earth; He$^+$ ions come to the more distant region, and, finally, proton fluxes are brought into the most distant region of the plasma sheet. To date, many experimental works are published in which data are presented on the detection of multicomponent fluxes of molecular ions in the polar ionosphere at altitudes ~ 10000 km (see, for example, [20]).

Let us consider now the measurements of ion energy distributions obtained outside the plasmasphere, at geocentric distances $\sim 3.9R_E$ ($L > 8.2$). As noted above, outside the plasmasphere, the instrument measured ion fluxes $\sim 10^5-10^7$ cm^{-2} s^{-1} with an energy of $\sim 10-20$ eV. However, it is evident from Fig. 3 that near the apogee of a number of orbits of Auroral Probe, the instrument measured, as a rule, one or several spectra of ion fluxes with flux values $\sim 5 \times 10^7-5 \times 10^8$ cm^{-2} s^{-1}. Figure 5 shows several differential energy spectra for such ion fluxes recorded in 5 passages of Auroral Probe near the apogee, in the pre-noon and dawn sectors of the magnetosphere in the period from September 9, 1996, to September 14, 1996. We can see from Fig. 5 that at $R_E = 3.9$ and $L > 8.2$, the measurement of energy spectra typical, according to ALFA-3 data, for the exoplasmasphere ($F < 10^7$ cm^{-2} s^{-1}, the energy of directed motion $E > 20$ eV) is suddenly interrupted, and instead, one or several spectra with many clear-cut maxima with $F > 5 \times 10^7$ cm^{-2} s^{-1} and the bulk velocity component normal to the analyzer entrance window and corresponding to $E < 0.5$ eV are measured. Thereafter, the recording of spectra with $E > 20$ eV is resumed. The spectra measured on September 9, 1996, at 2:41 UT, on September 11, 1996, at 15:21–15:24 UT, and on September 14, 1996, at 12:41, 12:44, and 18:43 UT have a common characteristic feature: the ratios of the positions of the 1st, 2nd, 3rd, and 4th maxima on the
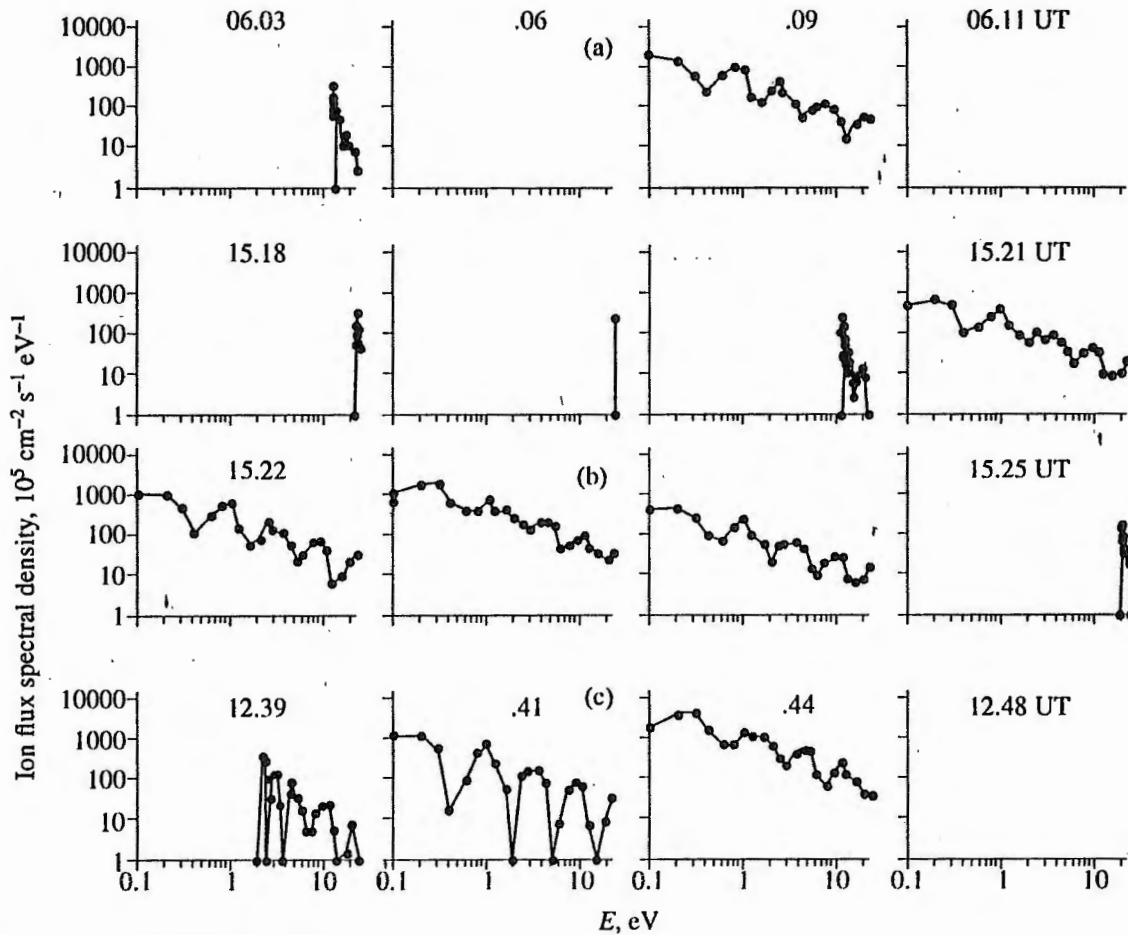
Fig. 5. Examples of multicomponent spectra measured at $R_E = 4$ at high latitudes. (a) September 9, 1996, 10.6–10.8 MLT, $R = 3.9R_E$, $L = 8.8–8.2$, $A = 134°–130°$; (b) September 11, 1996, 7.2–7.4 MLT, $R = 3.9R_E$, $L = 32–30$, $A = 110°–115°$; (c) September 14, 1996, 7.5–8.2 MLT, $R = 3.9R_E$, $L = 39–35$, $A = 172°–180°$.

energy scale in each spectrum (E_1, E_2, E_3, and E_4) are close to 1:4:16:32. This circumstance can be considered as an indication that the modulation analyzer of the ALFA-3 instrument, having recorded energy spectra with four maxima, thus measured the ion flux consisting of the following mixture of ions: H^+, He^+, $O^+ + N^+$, and $O_2^+ + N_2^+ + NO^+$. The table contains the values of ion fluxes He^+, $N^+ + O^+$, and $N_2^+ + O_2^+ + NO^+$, normalized to the flux of H^+ ions, and the total flux values for the multicomponent spectra presented in Fig. 5. The data on the partial fluxes in the table are given together with the UT values, geocentric distances, L coordinate, local magnetic time, and the maximum value of the K_p index for the day preceding the measurements. Attention should be drawn to the good agreement between the partial fluxes of the molecular ions measured by the ALFA-3 instrument on *Auroral Probe* and by the SMS instrument on the *EXOS-D* satellite [21] and to the significant discrepancy existing between the values of the total flux of molecular ions:

$> 10^7$ cm^{-2} s^{-1} in the first case and 10^5 cm^{-2} s^{-1} according to [21].

Bearing in mind that all measurements of multicomponent fluxes on *Auroral Probe* have been performed at high latitudes and at geocentric distances $\sim 4R_E$, these fluxes, as well as the polar wind fluxes, should be assigned to the magnetospheric phenomena related to the plasma outflow from the high-latitude ionosphere.

CONCLUSION

We can draw the following preliminary conclusions from the experimental data presented in this paper:

1. The ALFA-3 instrument, containing an analyzer with retarding potential and modulation analyzer, is an effective tool for measuring fluxes of low-energy ions inside and outside the plasmasphere. These instruments make it possible to determine reliably the instant of the plasmapause crossing by a satellite, by measuring the flux value and the component of bulk

Table

Date, 1996	UT	R, R_E	L	MLT	K_{pm}	F_{He^+}/F_{H^+}	$F_{N^+ + O^+}/F_{H^+}$	$F_{N2^+ + O2^+ + NO^+}/F_{H^+}$	$F, 10^8 \, cm^{-2} s^{-1}$
9 Sept.	6.09	3.9	8.6	10.7	2_-	0.48	0.22	0.06	3.1
11 Sept.	15.21					0.56	0.16	0.07	0.9
	15.22	3.9	30	07.4	5_-	0.48	0.16	0.06	1.5
	.15.24					0.49	0.14	0.06	0.7
14 Sept.	12.41	4.0	37	07.6		0.53	0.13	0.06	1.5
	12.44	3.9	35	08.1	4_0	0.30	0.12	0.05	5.6
	18.43	3.9	15	07.1		0.49	0.11	0.06	0.4

velocity of low-energy plasma, normal to the entrance window of the analyzer.

2. Experimental evidence is obtained for the existence of a region in the noon and midnight plasmasphere, adjacent to the plasmapause on the inside, where the velocity distribution of low-energy ion fluxes differs significantly from the Maxwellian. According to preliminary data, this region may coincide with geomagnetic tubes that are filled with ionospheric plasma after their devastation by a magnetic substorm. It is possible that the position of the inner boundary of this region coincides with the nearest-to-Earth position of the plasmapause, which was occupied by the latter during the substorm development.

3. In the region of the magnetosphere, immediately adjacent to the plasmapause on the outside, the fluxes of low-energy plasma (with energy in the range 9–25.5 eV) participating in the magnetospheric convection are systematically recorded.

4. At geocentric distances ~$4R_E$ ($8 < L < 30$), in the dawn sector of the magnetosphere, the energy spectra of ion fluxes with several maxima are sometimes recorded. The ratio of the energies of these maxima is close to the 1:4:16:32 ratio, which suggests that the multicomponent ion fluxes containing H^+, He^+, O^+, and $O_2^+ + N_2^+ + NO^+$ ions may sometimes exist above the polar cap, with the values $F > 5 \times 10^7 \, cm^{-2} \, s^{-1}$.

ACKNOWLEDGMENTS

REFERENCES

1. Gringauz, K.I., Bezrukikh, V.V., Ozerov, V.D., *et al.*, Investigation of Interplanetary Ionized Gas, Energetic Electrons, and Solar Corpuscular Radiation Using Three-Electrode Traps of Charged Particles aboard the Second Soviet Space Rocket, *Dokl. Akad. Nauk SSSR*, 1960, vol. 131, pp. 1301–1304.

2. Gringauz, K.I., The Structure of the Earth's Ionized Gas Envelope Based on Local Charged Particle Concentration Measured in the USSR, in *Space Res. 2, Proc. of the 2nd Int. Space Sci. Symp.*, N. Holland Publ. Co, 1961, pp. 574–592.

3. Whipple, E.C., Warnock, J.M., and Wincler, R.H., Effect of Satellite Potential in Direct Ion Density Measurement through the Plasmapause, *J. Geophys. Res.*, 1974, vol. 79, pp. 179–186.

4. Whipple, E.C., Potentials of Surfaces in Space, *Rep. Prog. Phys.*, 1981, vol. 44, pp. 1197–1250.

5. Olsen, R.C., The Hidden Ion Population of the Magnetosphere, *J. Geophys. Res.*, 1982, vol. 87, pp. 3481–3488.

6. Knott, K., Decreau, P., Korth, A., *et al.*, Observations of the GEOS Equilibrium Potential and Its Relation to the Ambient Electron Energy Distribution, in *Proc. of the 17th ESLAB Symp. "Spacecraft/Plasma Interaction...", Noordwijk, the Netherlands, Sept. 1983* (ESA SP-198, Publ. Dec. 1983).

7. Lindqvist, P.-A., The Potential of ISEE in Different Plasma Environment, *Ibid.*

8. DeForest, S.E., Spacecraft Charging at Geosynchrous Orbit, *J. Geophys. Res.*, 1972, vol. 77, pp. 651–659.

9. Decreau, P., Beghin, C., and Parrot, M., Global Characteristics of the Cold Plasma in the Equatorial Plasmapause Region, as Deduced from GEOS-1 Mutual Impedance Probe, *J. Geophys. Res.*, 1982, vol. 87, pp. 695–712.

10. Chappell, C.R., Moore, T.E., and Waite, J.H., Jr., The Ionosphere as a Fully Adequate Source of Plasma for the Earth's Magnetosphere, *J. Geophys. Res.*, 1987, vol. 92, pp. 5896–5910.

11. Moore, T.E., Origins of Magnetospheric Plasma, *Rev. Geophys. Sup.*, 1991, pp. 1039–1048.

12. Moldwin, M.B., Thomson, M.F., Bame, S.J., *et al.*, The Fine-Scale Structures of the Outer Plasmasphere, *J. Geophys. Res.*, 1995, vol. 100, pp. 8021–8029.

13. Banks, P.M., Nagy, A.F., and Axford, W.I., Dynamic Behavior of Thermal Protons in the Mid-Latitude Ionosphere and Magnetosphere, *Planet. Space Sci.*, 1971, vol. 19, pp. 1053–1061.

14. Grigoriev, S.A., Recovery Processes in Plasmasphere, *Kosm. Issled.*, 1991, vol. 29, pp. 85–94.

15. Horwitz, J.L., Comfort, R.H., and Chappel, C.R., Thermal Ion Composition Measurements on the Formation of the New Outer Plasmasphere and Double Plasmapause during Storm Recovery Phase, *Geophys. Res. Lett.*, 1984, vol. 11, pp. 701–704.

16. Axford, W.I., The Polar Wind and the Terrestrial Helium Budget, *J. Geophys. Res.*, 1968, vol. 73, pp. 6855–6863.

17. Banks, P.M. and Holzer, T.E., The Polar Wind, *J. Geophys. Res.*, 1968, vol. 73, pp. 6846–6858.

18. Hoffman, J.H. and Dodson, W.H., Light Ion Concentration and Fluxes in the Polar Regions during Magnetically Quiet Times, *J. Geophys. Res.*, 1980, vol. 85, pp. 626–632.

19. Lockwood, M. and Chandler, M.O., Horwitz, M.O., *et al.*, The Cleft Ion Fountain, *J. Geophys. Res.*, 1985, vol. 90, pp. 9736–9748.

20. Horwitz, J.L. and Lockwood, M., The Cleft Ion Fountain: a Two-Dimensional Kinetic Model, *J. Geophys. Res.*, 1985, vol. 90, pp. 9736–9748.

21. Yau, A.W., Whalen, B.A., Goodenough, C., Sagava, E., *et al.*, EXOS D (Akebono) Observations of Molecular NO^+ and N_2^+ Upflowing Ions in the High-Altitude Auroral Ionosphere, *J. Geophys. Res.*, 1993, vol. 98, pp. 11205–11224.